





Effects of Groove Angles and Quenchants on the Structural Integrity of a Single-Vee Butt Welded Joint of AISI 1024 Carbon Steel Weldment

Vincent Chukwuemeka Ezechukwu*, Joseph Awa Amogu and Kennedy Chinedu Owuama

Department of Mechanical Engineering, Chukwuemeka Odumegwu Ojukwu University Anambra State Nigeria.

*Corresponding author email: vc.ezechukwu@coou.edu.ng; Tel.: +234(0)8061393474

Abstract	Article History
<p>The high failure rate of welded structures has made it necessary to investigate some welding parameters that may be involved in these failures, such as groove angles, quenchants, welding current, welding voltage, and weld pass speed. This investigation aimed to investigate the impact of quenchants and groove angle on the structural integrity of a Single-V butt welded joint, using AISI 1024 steel. Nine samples, each measuring 150 x 80 mm, were cut from an 8 mm thick AISI 1024 steel plate. The findings of the study showed that, in comparison to oil and kerosene-quenched samples, the weldments cooled with natural air had significantly greater impact strength for the corresponding groove angles of 30°-130J, 45°-128J, and 60°-122J. Furthermore, out of all the groove angles taken into consideration in this study, the weldments of the samples that were cooled naturally had the highest hardness value; the maximum value of 188HBW was obtained with a groove angle of 60°. At groove angles of 45° and 60°, respectively, Mobil oil quenchant produced greater hardness values of 150HBW and 159HBW than kerosene, but at a groove angle of 30°, kerosene produced a larger hardness value of 152HBW than Mobil oil. Although the observed mechanical qualities varied across all samples due to the changes in the quantities of cementite and pearlite present in the samples, the microstructural inspection studies showed phases of cementite and pearlite structures on all samples. The study's conclusions will help structural industries achieve the best possible weldment performance for AISI 1024 carbon steel.</p> <p>Keywords: AISI 1024 Steel, Quenchant, Welding, Structures, Hardness, Corrosion</p>	<p>Received: 03 Jan 2025 Accepted: 10 Jan 2025 Published: 16 Jan 2025</p> <div style="text-align: center;">  <p>Scan QR code to view*</p> <p>License: CC BY 4.0*</p>  <p>Open Access article</p> </div>

How to cite this paper: Ezechukwu, V. C., Amogu, J. A., & Owuama, K. C. (2025). Effects of Groove Angles and Quenchants on the Structural Integrity of a Single-Vee Butt Welded Joint of AISI 1024 Carbon Steel Weldment. *IPS Journal of Engineering and Technology*, 1(1), 1–12. <https://doi.org/10.54117/ijet.v1i1.3>

1. Introduction

The high failure rate of welded structures has made it necessary to investigate certain weldment parameters that have a significant impact on the material's atomic arrangement and structural integrity. According to Ekengwu et al. [1], these weldment properties are what determine the quality and strength of the weld. According to [1], these variables include the type of welding that is used, the welding current and voltage, the type of base metals, the speed at which the weld passes are made, the type of filler material that is used, the type of cooling substances (quenchants), and the geometry and angular orientation of the weld groove. In regards to this concern, the performance characteristics of engineering materials—particularly carbon steel materials—under service conditions are entirely determined by their chemical composition, grain size, presence of defects, and other extrinsic factors [2]. Furthermore, the mechanical characteristics of carbon steels—such as their hardness, fatigue strength, ductility, strength, and formability—improve their performance while in service. According to Ajayi et al. [3] and Joesph et al. [4], inadequate engineering design, the

use of subpar materials, fabrication techniques, manufacturing faults, and fatigue problems may also be linked to the failure of carbon steel materials. While a number of welding techniques rely on heating with an electric arc, Shielded Metal Arc Welding (SMAW), or stick welding, is the most traditional and straightforward. In this procedure, an electrode holder that holds an electrode receives current from an electrical machine, which can be either DC or AC. The workpiece and the welding machine are connected by an earth connection, which gives the current a way to return. An electric arc is started when the electrode tip is tapped, or struck, against the workpiece to begin the weld. A molten pool and the electrode's end are produced practically immediately by the high temperature (6000–7000°C) that is produced [5]. The electrode fills the groove and keeps melting into the pool. While advancing the electrode along the joint, the machine operator must regulate the distance between the electrode tip and the workpiece. The Shielded Metal Arc Welding (SMAW) details diagram is displayed in Figure 1.

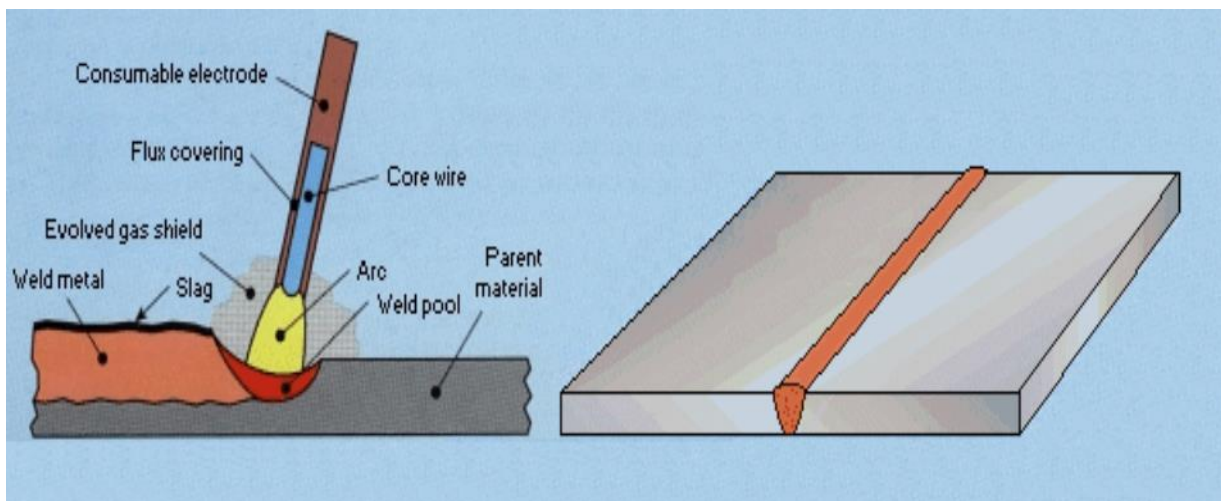


Figure 1: Shielded metal arc welding details [6]

An extruded coating of flux is applied to the electrode in the SMAW. In addition to the flux elements reacting with undesirable impurities like surface oxides to form a slag that floats to the top of the weld pool, the heat of the arc melts the flux, forming a gaseous shield to keep air out of the molten pool. This creates a crust that shields the weld from damage as it cools. The slag chips off when the weld cools. The slag generated during the welding process is shown in Figure 2.



Figure 2: A slag cut off from a welded metal plate [7]

The strength of AISI 1024 steel is medium. 1024 steel has good low-temperature properties, high cold-straining plasticity, and satisfactory weldability and machinability. Additionally, 1024 steel has a better quench-hardening capacity than carbon steel with a comparable carbon concentration. The crucial complete hardening diameters in oil range from 4 to 15 mm. However, 1024 steel is prone to overheating, decarburization sensitivity, and temper brittleness when heat treated. [8], studied how welding factors affected 304 SS and 316 in both TIG and MIG welding. The Taguchi approach has been used to achieve the best possible outcome. According to the data, the joint created using TIG welding has a higher ultimate tensile strength (675.22 MPa) than the sample created using MIG welding (652.029 MPa). Conversely, MIG-welded joints have a hardness of 196.54 BHN, and TIG-welded joints have a hardness of 162.53 BHN.

According to their research, [9] found that the X-type groove is stronger than the V-groove design. In addition, the highest strength is achieved in both tension and compression by X-type joints with an X groove (48 degrees) and weld joints with a V-groove geometry and a 54-degree groove angle.

Researchers [10] carried out an experimental work to study the influence of groove angle on the tensile strength and Charpy v-notch impact strength of mild steel weld joints. As per results, the maximum average tensile strength obtained is 513.68 MPa for joint-1 having a groove angle of 50, and the minimum tensile strength reported is 471.29 MPa for joint-3 having a groove angle of 30. Besides this, Charpy v-notch strength is highest (53.47 J) for joint -1 and minimum for joint 3.

Most welding parameters, including welding current, welding voltage, groove angle, cooling media, weld speed, etc., negatively affect the structural integrity of the weld joints of engineering materials (usually steel), their ability to withstand corrosion, and their microstructural patterns [11]. Studying the microstructural patterns and strength factors of steel welded joints that are mostly mild steel, as well as other weldments of different materials under the influence of individual or combination weld parameters, has been the main focus of research efforts [12]. Researchers have looked into how changes in welding current or voltage, weld speed, and other factors affect the structural integrity and microstructural patterns of steel welded joints [13]. The effects of several quenchants, such as brine solution, diesel, air, castor seed oil, neem seed oil, gmelina oil, palm oil, water, etc., on the weldments of either comparable or dissimilar steel material have also been studied. The impact of quenchants (natural air, vehicle engine oil, and kerosene oil) and groove angle variations on the hardness, impact strength, microstructural features, and corrosion resistance of a Single-V butt-welded joint of AISI 1024 structural steel material must thus be investigated. This research endeavor is also focused on determining the ideal groove angle and cooling medium to be used while welding steel. This was accomplished by using the optimization tool of the response surface approach.

2. Materials and Methods

2.1 Material

AISI 1024 structural steel, quenchant (natural air, Mobil lubricant oil (SAE 5W-30), and kerosene oil), emery paper (140 and 220), a filing machine, a milling machine, an atomic absorption spectrometer (AAS), grinding stone, filing machine cutters, an arc welding machine, welding electrodes (gauge 8), a Brinell hardness testing machine (Akb 3000M), an optical electron microscope, and software tools (Design Expert 11.0 software) were among the materials, substances, and equipment used in this study.

The steel was purchased from the Onitsha, Nigerian state of Anambra, steel market. In this study, nine (9) samples of this substance were used. Each sample was cut from an 8 mm plate of AISI 1024 steel to dimensions of 150 x 80 mm. The experimental design and response variable optimization were conducted using Design Expert 11.0 software. The response variables were graphed using Microsoft Excel to visually represent their behavioral patterns under the several treatment processes, including quenching and angular variations.

2.2 Research Method

Chemical analysis of the received steel material, experiment design, sample preparation in accordance with experimental design, fusion welding (electric arc welding) of the samples, application of quenchant to the weld zone on the samples, experimental determination of the structural integrity (hardness, impact strength, and corrosion resistance studies), and microstructural studies of the welded specimens and optimization are the foundation of the methodical procedures used in this study. The following is a detailed explanation of these procedures.

2.2.1 Chemical Analysis of AISI 1024 Structural Steel Material

Using the absorption of optical radiation by free atoms in the gaseous state, atomic absorption spectroscopy (AAS) is a quantitative spectro-analytical method for identifying chemical elements [14]. It makes advantage of the idea that light with a certain, distinct wavelength can be absorbed by atoms (and ions). The atom absorbs the energy (light) when this particular wavelength of light is present. The atom's electrons transition between their ground and excited

states. The concentration of the element in the sample can then be ascertained by measuring the amount of light absorbed. The AISI 1024 steel that was received was characterized using an atomic absorption spectrometer to determine its % constituent makeup. To prevent dirt from interfering with the experiment, the specimen was first cleaned and polished. After that, a spark was added, and it was put inside the atomic absorption spectrometer. After starting the spark, the weight percentages of the components in the sample were recorded.

2.2.2 Design of Experiments

Design specialist The 2 objectives of the 11.0 software package are the development of Response Surface Methodology (RSM) and Design of Experiments (DOE). A group of statistical and mathematical methods for creating empirical models is known as response surface methodology, or RSM. Optimizing a response (output variable) that is impacted by multiple independent variables (input variables) is the goal of carefully planned experiments. The response can be graphically depicted as contour plots that aid in visualizing the response surface's form or in three dimensions. RSM is most widely used in specific scenarios where a number of input variables may have an impact on a process's quality attribute or performance metric. As a result, the response is a quality feature or performance metric. The input variables, often referred to as independent variables, are under the scientist's or engineer's control. The field of response surface methodology includes optimization techniques to determine the values of the process variables that yield desired response values, empirical statistical modeling to establish a suitable approximating relationship between the yield and the process variables, and experimental strategy to explore the space of the process or independent variables. The independent and response variables listed below were used in the experimental design that was carried out using the best (custom) design tool of the response surface approach.

Independent variables: Groove angles ((Fixed variable): 30°, 45° and 60°

Quenchant/Cooling media: natural air, lubricant oil (Mobil Lubricant oil SAE 5W-30) and Kerosene oil

Response Variables: Impact strength, corrosion rate, and hardness of the welded structures.

The experimental design is shown in table 1.

Table 1: Design of Experiment

Run	Sample ID	Factor 1 A: Groove angles Degrees	Factor 2 B: Quenchant	Response 1 Impact Strength Joules	Response 2 Hardness HBW	Response 3 Corrosion Rate cm/hr.
1	Sample A	30	Natural air			
2	Sample B	45	Natural air			
3	Sample C	60	Natural air			
4	Sample D	30	Mobil Lubricant oil SAE 5W-30			
5	Sample E	45	Mobil Lubricant oil SAE 5W-30			
6	Sample F	60	Mobil Lubricant oil SAE 5W-30			
7	Sample G	30	Kerosene oil			
8	Sample H	45	Kerosene oil			
9	Sample I	60	Kerosene oil			

2.2.3 Sample Preparations According to the Experimental Design

Using a file machine, the samples were initially cut off from an 8 mm thick plate of AISI 1024 steel material that measured 150 mm by 80 mm. Nine (9) samples in all were removed from the plate. Using a milling machine and a protractor for angular measurement, Single-V grooves with angles of 30°, 45°, and 60° were made on the nine cut-out samples. All nine (9) samples were produced with a root gap of 2 mm. The milled pieces' uneven dimensions were eliminated using a filing machine. All of the samples were then gently cleaned of rust, grime, etc., using emery sheets. To keep the samples smooth and prepared for welding, 140 roughness was applied first, then 220 roughness. The root gap, groove angle orientation, and sample dimensions are displayed in Figure 3 along with the sample's geometric configuration.

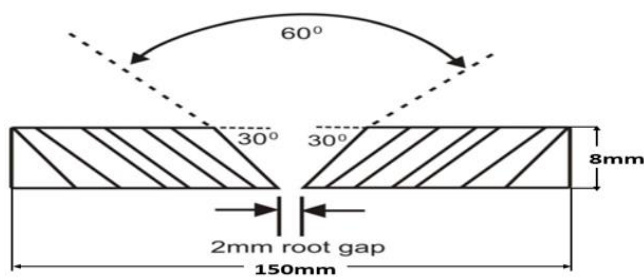


Figure 3: Geometric configuration of the samples

2.2.4 Welding of the Samples

Nine samples produced at their respective grooves using gauge 8 electrodes were welded using an electric arc welding machine. The Samurai E6013 electrode, which had conventional dimensions of 3.2 (1/8" × 320 mm), was utilized. Throughout the welding process, the arc welding voltage and current, which were 220V and 180A, remained consistent.

2.2.5 Application of Quenchants to the Samples

Three samples were left to cool naturally in the air following the welding operation, three more were quenched right away using the Lubricant oil, and the final three were quenched right away using kerosene oil. The samples were quenched, namely at the butt joints, which are the weld joints.

2.2.6 Optimization of the Responses

The measured responses were entered into the experimental design and optimized following the evaluation of the samples' mechanical characteristics. For this exact goal, a response surface methodology (RSM) numerical optimization tool was employed. In order to determine the greatest combination of factors that would produce the most dependable and optimal response parameters for a guaranteed welded quality of the samples, the responses were optimized. Table 2 shows the optimization criteria/goals used in the procedure.

Table 2: Optimization Criteria/Goals

S/N	Variables	Goals
1	Groove angle	In range
2	Quenchants	In range
3	Impact strength	Maximize
4	Hardness	Minimize
5	Corrosion rate	Minimize

2.2.7 Corrosion Resistance Studies

The corrosive behavior of a material is directly related to its strength. The experimental determination of the combinatorial effects of quenchant type and groove angles on the corrosion resistance performances of the prepared samples of AISI 1024 steel material is therefore necessary. Using the gravimetric (weight-loss) approach, the corrosion resistances of nine produced samples of welded steel were examined in a corrosive atmosphere with a 2M concentration of HCl. A piece of the nine samples' weldments measuring 21 mm x 12 mm x 8 mm was taken out of the initial welded and quenched samples. These cut sections were measured with a digital scale (with an accuracy of 0.01 mg) and ensured to be of the same weight prior to their introduction to the corrosive medium, 2M HCl. The area of each of the cut sections was 252mm². Each of the samples was dropped in 2M concentration of HCl at ambient conditions and was allowed to stay for 3 days (72 hours), and thereafter the samples were taken out, cleaned with distilled water, and reweighed. The corrosion rate (C_r) was calculated by using the following equation [15]:

$$C_r = \frac{87.6 \times w}{atd} \quad (1)$$

Where:

t = the exposure time in hours (72 hrs.)

a = the area of the exposed steel sample (cm²)

w = weight loss in grammes (g)

d = density of the steel material (= 7.87 g/cm³)

2.2.8 Microstructural Examination /Studies

To visualize the crystal structures and grain distribution of the material that contributed to the observed properties of the weldments, the optical electron microscope was used to examine the microstructural features and grain patterns of all the welded steel samples (both the HAZ and weldments).

3. Results and Discussion

3.1 Chemical Compositions of the As-received AISI 1024 Carbon Steel

Table 3 presents the major elemental compositions of AISI 1024 carbon steel just as received from the steel market, Onitsha, Anambra State, Nigeria.

Table 3: Chemical compositions of AISI 1024 carbon steel

Elements	Carbon	Iron	Manganese	Phosphorous	Sulphur
Symbols	C	Fe	Mn	P	S
Contents (%)	0.20	99.27	0.45	0.03	0.05

Table 3 makes it evident that iron was the most abundant elemental constituent in AISI 1024, with a 99.27% percentage presence and a low carbon concentration of 0.2%.

3.2 Examination of the Mechanical Properties of the HAZ and Weldments

Figure 4 shows how quenchants and changes in groove angle affect the impact strength of AISI 1024 weldments.

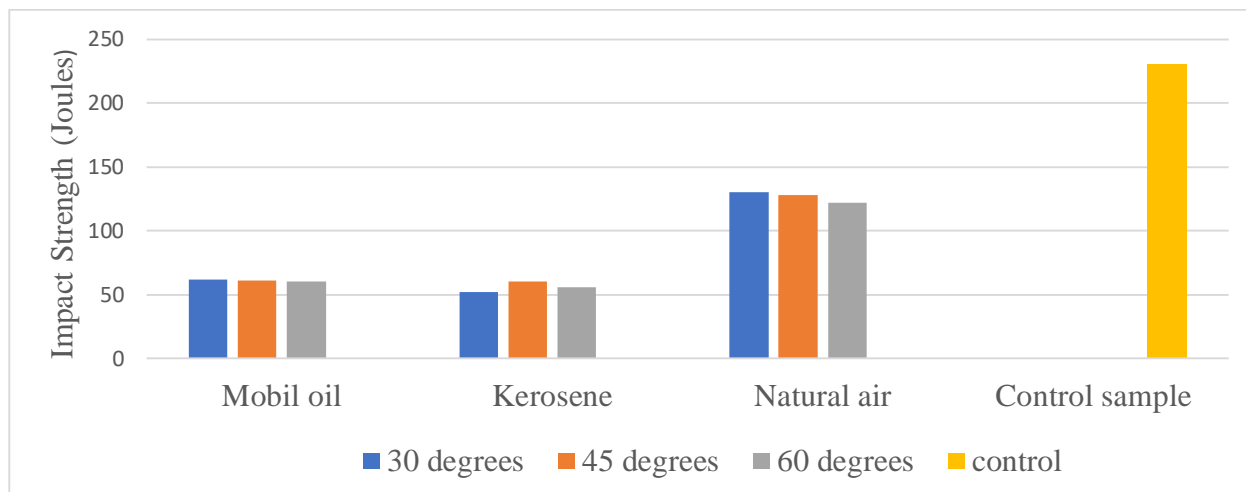


Figure 4: Multiple bar chart showing the effect of groove angle and quenchants on the impact strength of AISI 1024 weldments

Figure 4 shows that, in comparison to oil and kerosene quenched samples in their study, the weldment cooled with natural air had a significantly greater impact strength for the corresponding groove angles of 30°-130J, 45°-128J, and 60°-122J [6]. This may be explained by the sample molecules' consistent configuration, which results from natural cooling. Additionally, the oil-quenched sample's impact strength values differed widely, with the greatest value of 62J being obtained at a groove angle of 30°. Likewise, at a 45° groove angle, the kerosene-quenched samples yielded the greatest impact strength of 60J, with values of 52J and 56J at 30° and 60°,

respectively, closely correlated. Thus, the applied welding variables, groove angles, and quenchants proved to have a significant effect on the impact strength of AISI 1024 carbon steel [16]. Figures 5 and 6 show the effects of the welding variables groove angles and quenchants on the hardness factor of AISI 1024 weldments and the HAZ of the samples, respectively. The experiment's control sample produced an impact strength value of 230 J. Additionally, the results obtained confirm that a groove angle of 30° is relatively suitable for good impact strength actualization for AISI 1024 weldments.

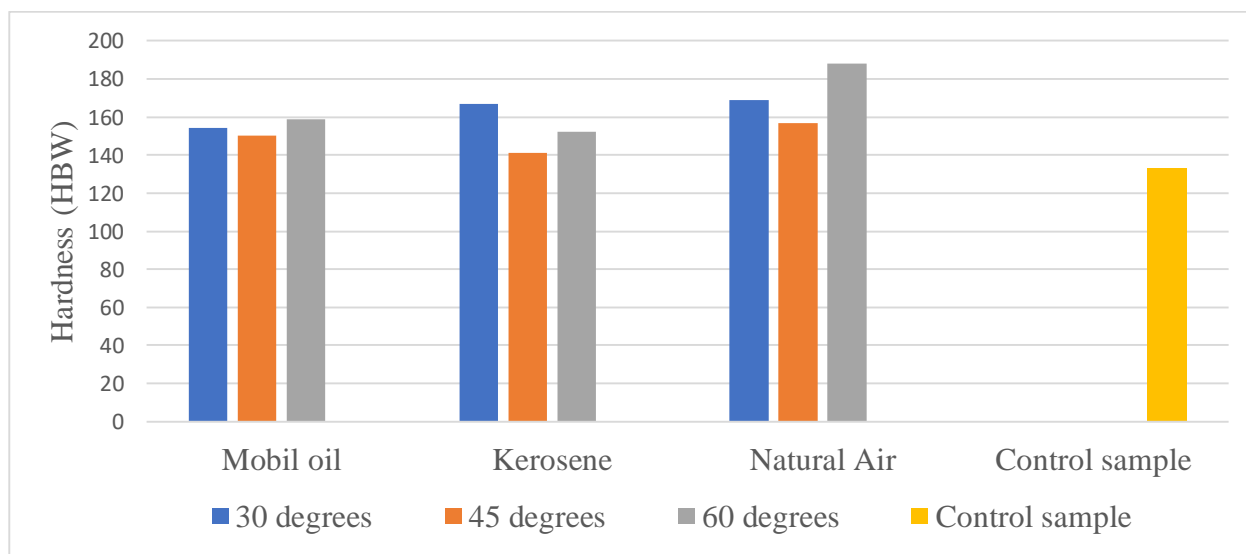


Figure 5: Multiple bar chart showing the effect of groove angle and quenchants on the hardness property of AISI 1024 carbon steel weldment

Figure 5 indicates that, out of all the groove angles taken into consideration in this investigation, the weldments of the samples cooled with natural air had the highest hardness value, with a groove angle of 60° producing the highest value of 188HBW. This might be because the samples were uniformly cooled, which led to the correct distribution and production of the air-cooled samples' molecules as well as the layout of the grain boundaries. Additionally, kerosene created a bigger hardness value of 152HBW than the lubricant oil at a groove angle of 30°, while the lubricant oil quenchant produced higher

hardness values of 150HBW and 159HBW at 45° and 60°, respectively. The control sample had the lowest hardness comparatively to all the weld situations presented [17]. The development of martensite structure, which is known to be a structure of high hardness value, on the quenched samples (oil and kerosene quenched) is what caused the enhanced hardness of the samples ([5], [18]). The hardness of the AISI 1024 carbon steel material's weld is thus influenced by the type of quenchant and groove angles, as these observations confirmed.

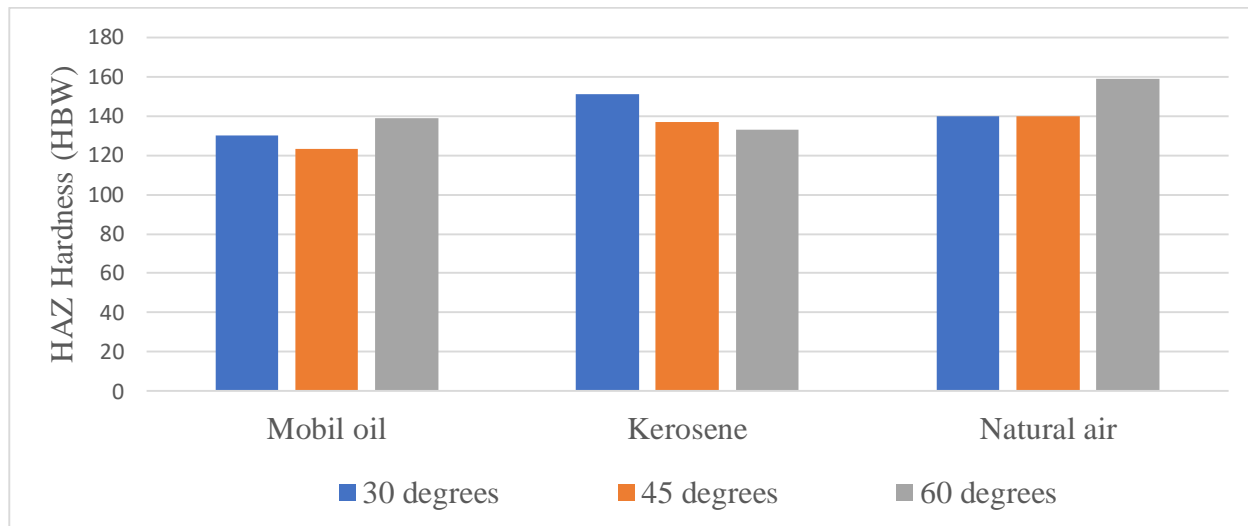


Figure 6: Multiple bar chart showing the effect of groove angle and quenchants on the hardness property of AISI 1024 carbon steel HAZ.

Furthermore, figure 6 indicates that, when compared to other quenchants used, the HAZ of the air-cooled sample at a groove angle of 60° had the highest hardness value of 159HBW. The HAZ hardness value of 140 HBW was higher in air-cooled samples with groove angles of 30° and 45° than in oil- and kerosene-quenched samples with groove angles of 30/45° and 45/60°, respectively. With the exception of the oil-quenched sample, which had a groove angle of 45° and may have resulted from a deformed molecular arrangement of the sample's lattice structural pattern, the HAZ hardness of all the quenchants employed was noticeably higher than the hardness of the control sample [5].

3.3 Corrosion Resistance Studies of the Samples Weldments

Figure 7 shows that the samples quenched with kerosene oil and Mobil lubrication oil exhibit higher rates of corrosion than

the samples cooled by natural air. Furthermore, it was found that as the groove angle increased, so did the corrosion rate. This was due to the fact that the weld bead size and the groove angle are linearly related; that is, when the groove angle increases, the weld bead dimension will likewise grow, creating a larger welded area of the sample that will be exposed to the corrosive media. The increased corrosion rates found for Mobil lubrication oil and kerosene-quenched samples are also explained by the fact that oil application is recognized to be one of the factors that influences corrosion mechanics because of its chemical makeup. Furthermore, when exposed to a corrosive environment, the percentage decrease in sample weight from the control to the kerosene oil-quenched samples varied between 6 and 24 percent. The type of joint preparation used may possibly be responsible for this high rate of weight loss.

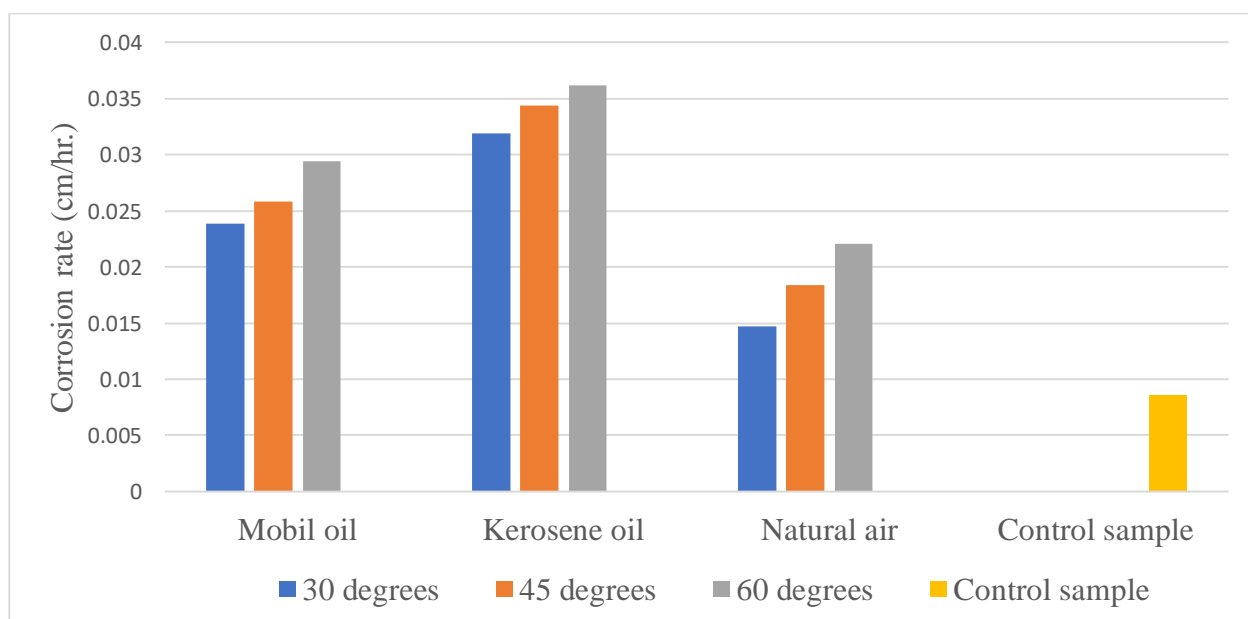


Figure 7: Corrosion rate of AISI 1024 carbon steel weldments at varying groove angles and quenchants in 2M of HCl medium

3.4 RSM Optimization of the Responses

The RSM optimization tool was used to determine the ideal factor circumstances, or input factors, groove angle and quenchant, that would produce the best response characteristics. Nine (9) different solutions were found using

the central composite design (CCD) optimization (RSM) tool; nonetheless, the solution with the highest attractiveness value (0.775) was selected as the best option. The desirability plots in Figures 8–9 provided information on the ideal factor combination that would produce the best response values.

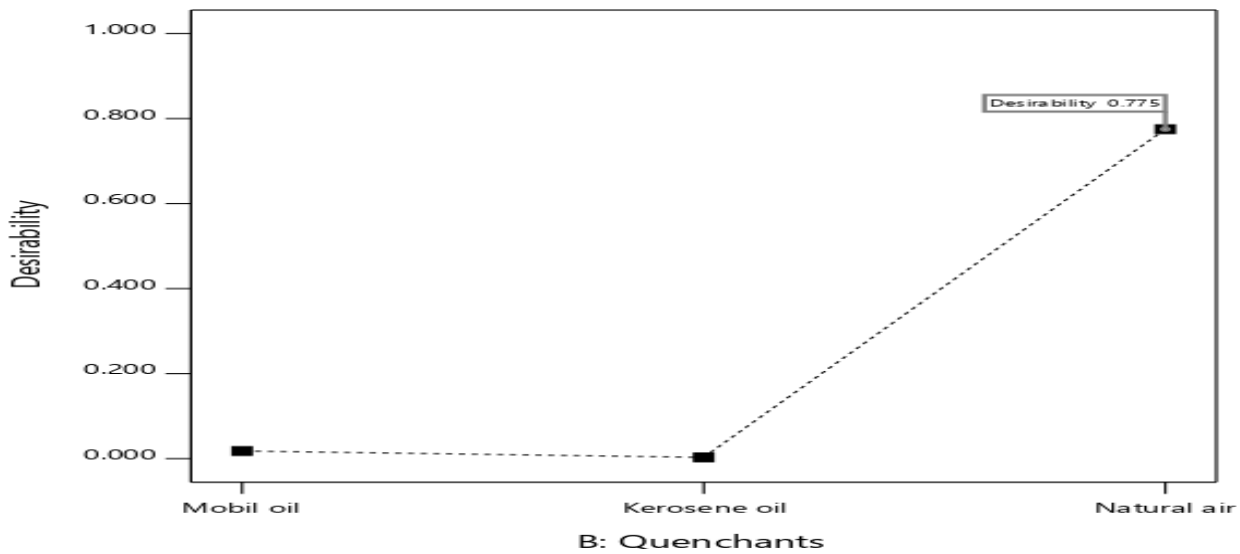


Figure 8: Desirability plot indicating the optimal quenchant that yielded the highest desirability value

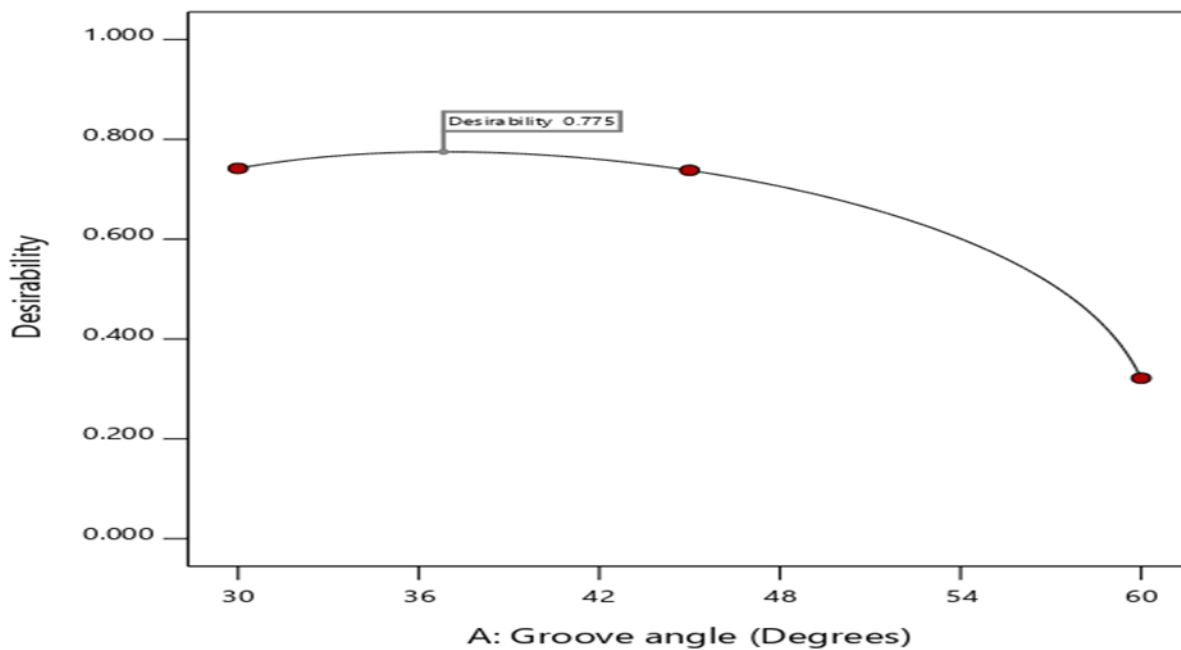


Figure 9: Desirability plot indicating the optimal groove angle with the highest desirability value

From figures 8-9, natural air and a groove angle of 36.8253 obtained at this optimal design solution/point are vividly could be observed as the optimal design point. The optimum presented in figures 10-12 respectively. response values- impact strength, hardness, and corrosion rate

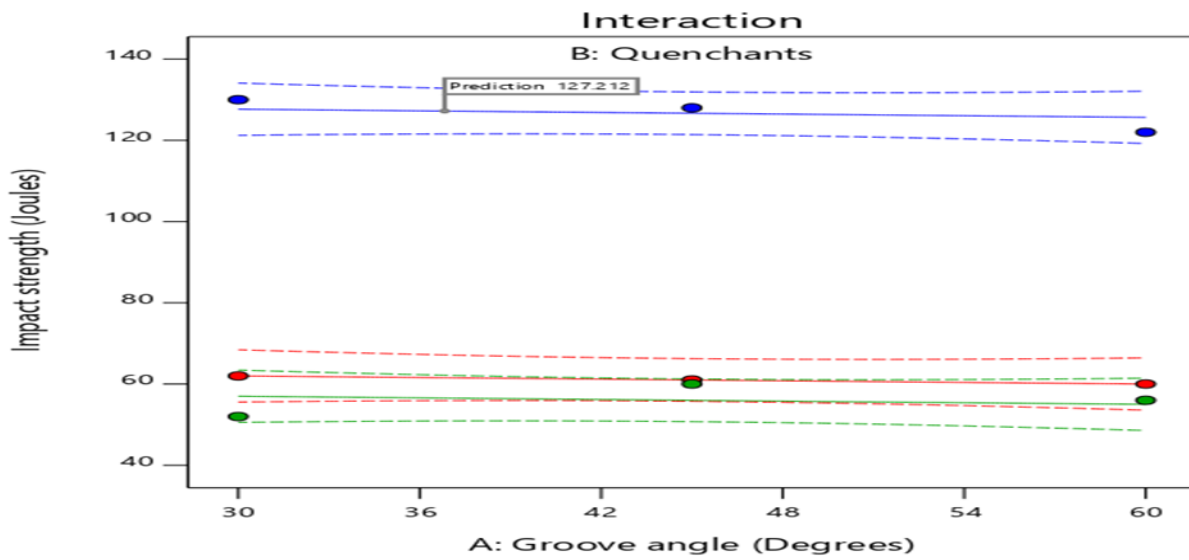


Figure 10: Maximized impact strength of the weldments at optimum design point

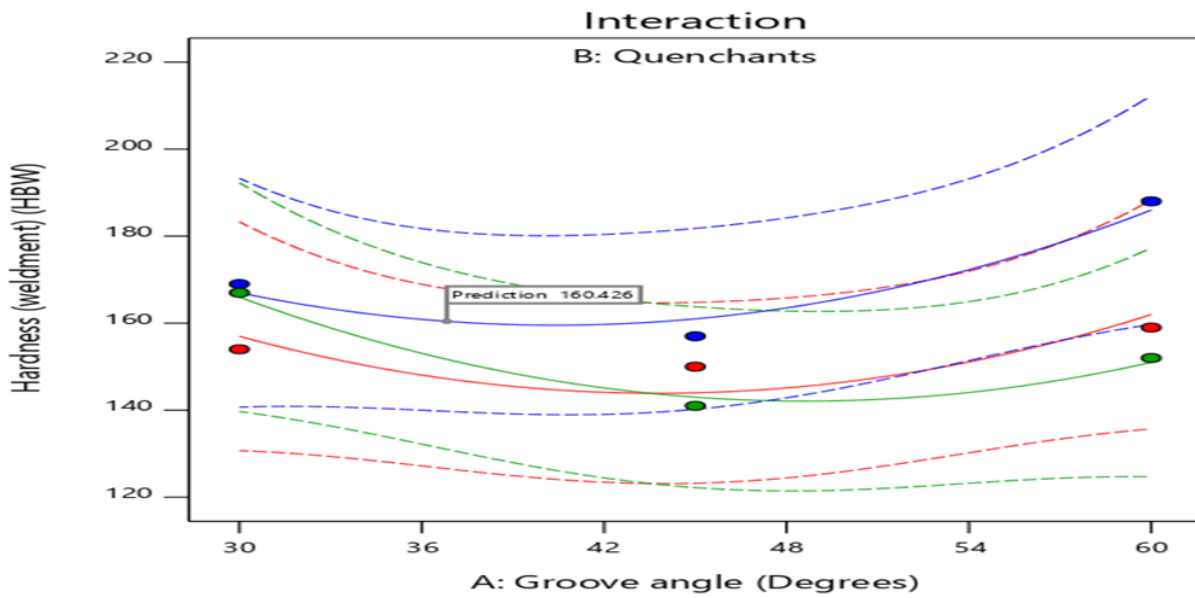


Figure 11: Minimized weldment hardness at optimum design point

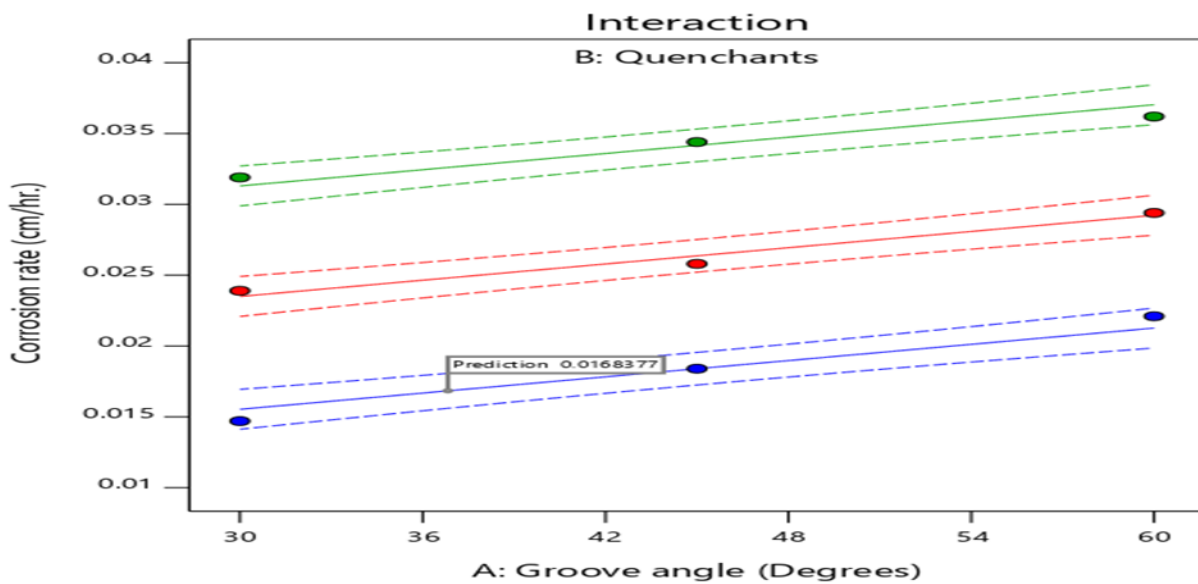


Figure 12: Minimized corrosion rate of the weldment at optimum design point/condition

The optimized response values, which are impact strength, cm/hr, 160.426 HBW, and 127.212 J, respectively. The hardness (weldment), and corrosion rate obtained at the ideal summary statistics of the responses at the optimum design condition/point, are shown in figures 10-12 as 0.01684 conditions are shown in Table 4.

Table 4: Summary statistics of the responses at the optimum design point

Solution	Predicted Mean	Predicted Median	Std Dev	SE Mean	95% CI low for Mean	95% CI high for Mean	95% TI low for 99% Pop	95% TI high for 99% Pop
Impact strength	127.212	127.212	3.54024	2.19047	121.581	132.842	103.746	150.678
Hardness(weldment)	160.426	160.426	6.48074	4.80695	139.744	181.109	72.6826	248.17
Corrosion rate	0.0168377	0.0168377	0.000775457	0.000479803	0.0156044	0.0180711	0.0116977	0.0219777

3.5 Microstructural Examination of the Weldments

The results of the microstructural examination of the weldment and HAZ for all the samples labelled A-I are presented in figures 13-15.

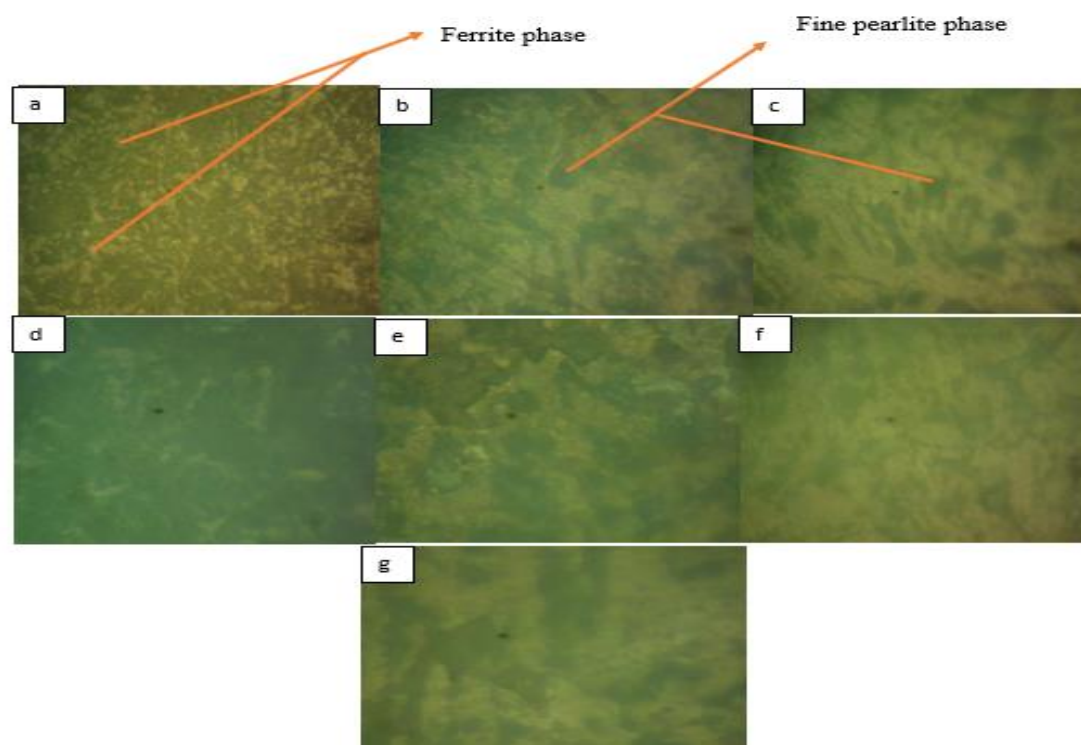


Figure 13: Microstructural examination at $\times 300$ magnification for (a) control sample (b) sample A weldment (c) sample B weldment (d) sample C weldment (e) sample A HAZ (f) sample B HAZ (g) sample C HAZ.

The control sample's microstructural features, as well as the weldments and HAZs of samples A–C, are shown in Figure 13. The control sample in figure 13a showed ferrite phases, which are frequently seen in low-carbon steels [20]. Iron makes up the majority of the ferrite structure, with little to no carbon. Rapid cooling prevents it from hardening. The fine pearlite structures that make up the steel samples' observable mechanical properties, such as impact strength and hardness, were revealed by air cooling of the samples, as shown in

figures 13b–13g. A blend of approximately 87.5% ferrite and 12.5% cementite arranged in alternate layers makes up pearlite, according to [20]. Furthermore, the air-cooled sample's high hardness property may have been caused by the presence of more cementite and pearlite structures in its composition [21]. Furthermore, slower cooling results in a coarser structure than faster cooling, which explains the air-cooled samples' reported mechanical characteristics.

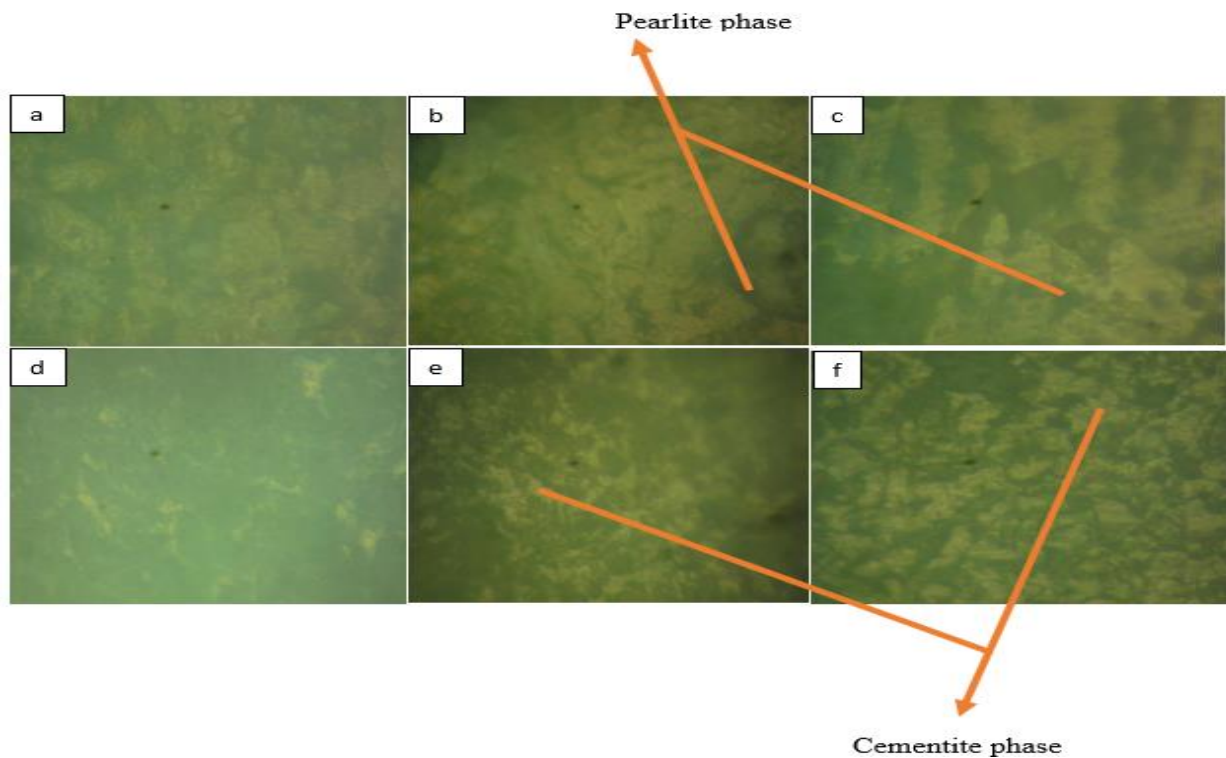


Figure 14: Microstructural examination at $\times 300$ magnification for (a) sample D weldment (b) sample E weldment (c) sample F weldment (d) sample D HAZ (e) sample E HAZ (f) sample F HAZ.

Figure 14 displays the microstructural examination of the weldment and HAZs of samples D-F. Finer pearlite and cementite structures/phases could be observed in figure 14. These phases contributed to the observed mechanical properties of the Mobil oil-quenched samples, which are impact strength and hardness properties. Also, the dispersion of these phases appears to be more uniform as the groove angle increases. These could be because of higher boundary provisions for homogenous solidification of the phases at larger groove angles.

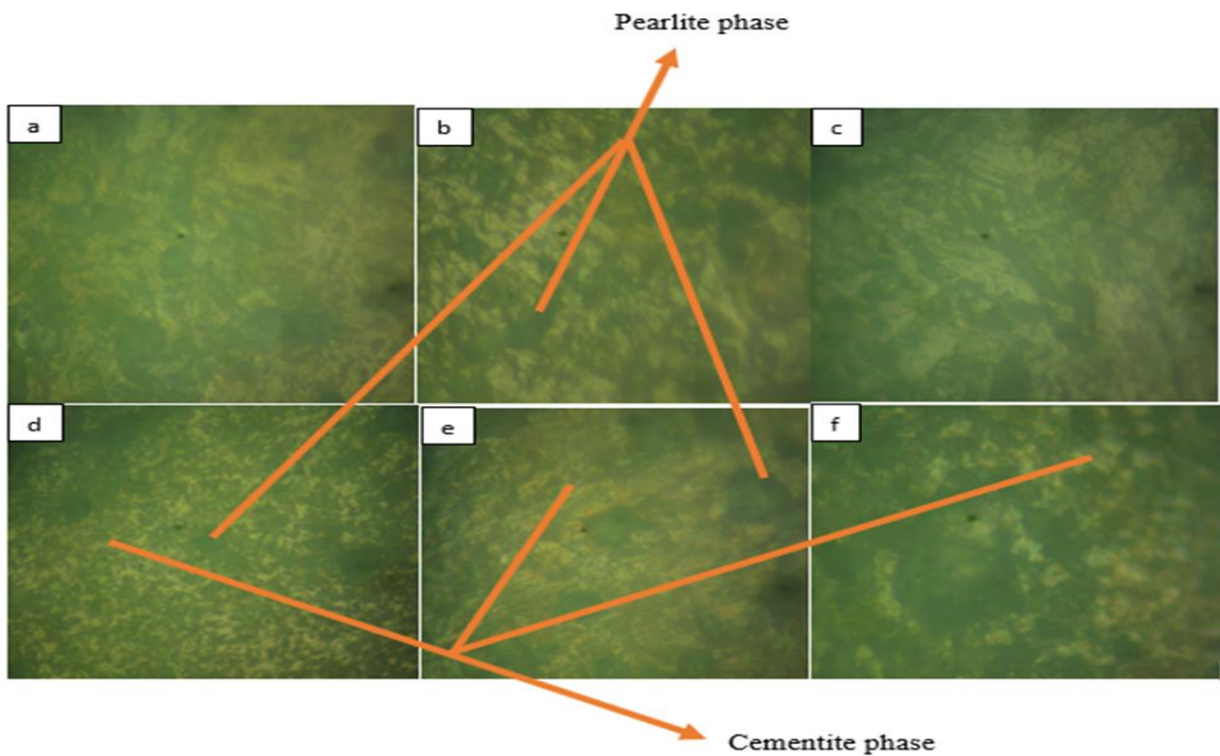


Figure 15: Microstructural examination at $\times 300$ magnification for (a) sample G weldment (b) sample H weldment (c) sample I weldment (d) sample G HAZ (e) sample H HAZ (f) sample I HAZ.

Figure 15 depicts the microstructural examination of the weldments and HAZs of samples G-I. The presence of pearlite and cementite phases was observed in the samples as displayed in figure 15. Cementite, according to [22], is a carbide of iron, which is extremely hard and generally increases with the carbon percentage present in the steel samples. The presence of pearlite and cementite phases in the samples explains the observed mechanical properties of samples G-I.

4. Conclusion

This study looked into how quenchants and groove angle affected the mechanical characteristics of a single v-groove butt welded joint made of AISI 1024 carbon steel, namely its impact strength and hardness. It is possible to make the following conclusion:

1. When compared to Mobil lubricant oil SAE 5W-30 and kerosene-quenched samples, the impact strength of the natural air-cooled weldment was noticeably higher for the corresponding groove angles of 30°–130J, 45°–128J, and 60°–122J.
2. The Mobil lubricant oil-quenched samples had a close range of values of impact strength, though the highest was achieved at a groove angle of 30° with a value of 62J. Similarly, the kerosene-quenched samples gave the highest value of impact strength of 60J at a groove angle of 45°, with closely related values of 52J and 56J at 30° and 60°, respectively. The experiment's control sample had an impact strength of 230 J. Furthermore, the results show that for AISI 1024 weldments, a groove angle of 30° is reasonably appropriate for good impact strength actualization.
3. For all of the groove angles taken into consideration in this investigation, the hardness integrity of the samples' weldment cooled with natural air was found to have the highest hardness value, with a groove angle of 60° producing the highest value of 188HBW. Additionally, kerosene created a larger hardness value of 152HBW than Mobil oil at a groove angle of 30°, whereas Mobil oil quenchant produced higher hardness values of 150HBW and 159HBW at 45° and 60°, respectively.
4. The formation of the martensite structure, which is known to be a structure of high hardness value, on the quenched samples (oil and kerosene quenched) is what caused the improved hardness.
5. The corrosion rates of the natural air-cooled samples were lower than those of the Mobil and kerosene oil-quenched samples. Furthermore, it was found that as the groove angle increased, so did the corrosion rate. Additionally, compared to samples quenched with kerosene, those quenched with Mobil oil exhibited a decreased rate of corrosion. This occurred because Mobil lubrication oil's chemical characteristics were incorporated into the weldments, improving its corrosion resistance over kerosene-quenched samples.
6. The optimal design conditions of groove angle (36.8253) and quenchant (natural air cooling) were determined by the central composite design (CCD) optimization to be the best factor combination that would result in the best response characteristics of a weld product. The impact strength, hardness, and corrosion rate at this ideal design point were

0.01684 cm/hr, 160.426 HBW, and 127.212 J, respectively.

7. The microstructural examination studies revealed phases of pearlite and cementite structures in all the samples, though the observed mechanical properties differed in all the samples due to the variations in the proportions of pearlite and cementite available in the samples. Also, the dispersion of these phases appears to be more uniform as the groove angle increases. These could be because of higher boundary provisions for homogenous solidification of the phases at larger groove angles

Author contribution

All the authors contributed to the development of the work.

Data availability

The authors confirm that the data supporting the findings of this study are available within the article

Consent for publication

The authors give the publisher the consent to publish the work.

Informed consent

The work does not require informed consent in the research.

Competing interests

The authors declare no competing interests.

References

- [1] Ekengwu, I.E., Okafor, O.C., Olisakwe, H.C., and Ugonna, U.D. (2021). Reliability centered optimization of welded quality assurance. *Journal of Mechanical Engineering and Automation*, 10(1):1-11.
- [2] T.T. Braide, C.C. Nwobi-Okoye, V.C. Ezechukwu. Microstructural and Electrochemical study of Value-added Al-Si-Mg alloy reinforced with synthesis carbon nanotube and periwinkle shell nanoparticles for brake disc application, *Chemical Data Collections*, Volume 39, 2022, 100878, ISSN 2405-8300, <https://doi.org/10.1016/j.cdc.2022.100878>.
- [3] Ajayi, J. A., Joseph, O.O., Oloruntoba, D.T. and Joseph, O.O. (2013). Experimental Failure Investigation of an Aircraft Nose Landing Gear", *International Journal of Metallurgical and Materials Engineering* 3 (1), 85-92.
- [4] Joseph, O.O., Abidakun, O. A., Aniyikaye, A. O. & Folorunsho, O. O. (2013), "Investigations on the material efficacy of failed helical gears in a gear train. *Industrial Engineering Letters* 3 (6), 46-54.
- [5] Khurmi, R.S., and Gupta, J.K., (2012). A textbook of workshop technology (manufacturing processes), Uttrakhand, published by Nirja publishers and printers (p) Ltd, pp 287-323Kopeliovich, D. (2008). *Classification of Welding Processes*.
- [6] Ikumapayi, O.M., Okokpujie, I.P., Afolalu, S.A., Ajayi, E.T., and Bodunde, O.P. (2018). Effects of quenchants on impact strength of single-see butt welded joint of mild steel. The 1st International Conference on Engineering for Sustainable World (ICESW), IOP Conf. Series: Materials Science and Engineering, vol. 391, pp. 1-11.
- [7] Ezechukwu, V. C., Braide, T. K., & Nwobi-Okoye, C. C. (2024). Multi-Response Optimization of Stir Casting Parameter of New Nanocomposites Formulation of Al-Si-Mg Alloy Reinforced with Synthesis Carbon Nanotube and Periwinkle Shell Nanoparticles via Taguchi-Grey Approach. *International Journal of Science and Engineering Invention*, 10(10), 71–81. <https://doi.org/10.23958/ijsei/vol10-i10/276>

- [8] Kumar, S. L., Verma, S.M., Prasad, Radhakrishna, P., kumar P.K., Shanker, T.S., (2011). Experimental investigation for welding aspects of AISI 304 & 316 by Taguchi technique for the process of TIG & MIG welding, International Journal of Engineering Trends and Technology- Volume 2, Issue 2, PP. 28-33.
- [9] Ipek Nazli Ezgi, Elaldi Faruk (2012). Analysis of welding groove angle and geometry on strength of armor steel, Materials and manufacturing processes, Vol. 2, pp.1437-1441, DOI: 10.1080/10426914.2012.709343.
- [10] Singh, T., Shahi, A.S., and Kaur, M., (2013). Experimental studies on the effect of multipass welding on the mechanical properties of AISI 304 stainless steel SMAW joints, International Journal of Scientific & Engineering Research, Vol.4, PP. 951-960.
- [11] Braide T. Kelsy, Chidozie Chukwuemeka Nwobi-Okoye, Vincent Chukwuemeka Ezechukwu, Remy Uche., Multi objective optimization of novel Al-Si-Mg nanocomposites: A Taguchi-ANN-NSGA-II Approach, Journal of Engineering Research, 2023, ISSN 2307-1877, <https://doi.org/10.1016/j.jer.2023.10.008>. (<https://www.sciencedirect.com/science/article/pii/S2307187723002687>)
- [12] Braide, T.K., Nwobi-Okoye, C.C. & Ezechukwu, V.C. Taguchi-Grey multi-response optimization of wear parameter of new nanocomposite formulation of Al-Si-Mg alloy reinforced with synthesis carbon nanotube and periwinkle shell nanoparticles. *Int J Adv Manuf Technol* **120**, 8363–8375 (2022). <https://doi.org/10.1007/s00170-022-09163-7>
- [13] Erebugha, Y., Kennedy, C., Ezechukwu, V.C. (2024). CORROSION INHIBITION OF DENNETTIA TRIPETALA ON ALUMINUM IN ALKALINE (NaOH) SOLUTION MEDIUM. *International Research Journal of Modernization in Engineering Technology and Science*. 6. 3565-3573. 10.56726/IRJMETS48913.
- [14] Ezeugo, J. O., Onukwuli, O. D., Ikebodu, K. O., Ezechukwu, V. C., & Nwaeto, L. O. (2019). Investigation of Akuamma Seed Extract on Corrosion Inhibition of Aluminum in Hydrochloric Acid Pickling Environment. *Earthline Journal of Chemical Sciences*, 1(2), 115-138. <https://doi.org/10.34198/ejcs.1219.115138>
- [15] Ezeugo JO, Onukwuli OD, Ikebodu KO, Ezechukwu VC, Nwaeto LO (2019) Optimization of Chrysophyllum albidum leaf extract as corrosion inhibitor for aluminium in 0.5 M H2SO4. *World Sci News* 125:32–50
- [16] Talabi, S.I., Owolabi, O.B., Adebisi, and J.A., Yahaya, T., (2017). Effect of welding variables on mechanical properties of low carbon steel welded joint. *Advances in Production Engineering & Management*. 9(4): 181–186.
- [17] Duan, Z., Li, Y., Zhang, M. *et al.* Effects of quenching process on mechanical properties and microstructure of high strength steel. *J. Wuhan Univ. Technol.-Mat. Sci. Edit.* **27**, 1024–1028 (2012). <https://doi.org/10.1007/s11595-012-0593-1>
- [18] Ezechukwu, V, C. (2024). Hybridization Effect on Thermo-mechanical Behaviour of Epoxy/breadfruit Seed Shell Ash Particles and Momordica Angustisepala Fiber Composites for High- temperature Devices Application. *Proceedings of the IRE*. Volume 7. 2456-8880. <https://www.irejournals.com/formatedpaper/1705783.pdf>
- [19] Sulaiman, S.A., Addullah, B., Alias, S.K., Ahmad, N.N., and Aziz, N.A. (2019). Investigation of corrosion rate of different types of welding joints using metal arc welding (SMAW). *IOP Conference Series: Materials Science and Engineering*, vol. 834, pp. 1-8.
- [20] Ezechukwu, V.C., Nwobi-Okoye, C.C. & Atanmo, P.N. Surface modification of *Momordica angustisepala* fiber using temperature-activated amino-functionalized alkali-silane treatment. *Int J Adv Manuf Technol* **109**, 1397–1407 (2020). <https://doi.org/10.1007/s00170-020-05697-w>
- [21] Nnaji, N B., Owuama, K C., Ezechukwu, V C. Microstructural and Chemical Analysis of Polypropylene/Pig-Bone-Ash/Hamburger Seed Shell Composite. *International Journal of Progressive Research in Engineering Management and Science (Ijprems)*. Vol. 04, Issue 12, 2583-1062(2024). DOI: <https://www.doi.org/10.58257/IJPREMS35744>
- [22] V. E. Ezechukwu, C. C. Nwobi-Okoye, I. U. Onyenanu. (2015) Analysis of Waste Gases at INTAFAC T Beverages, Onitsha – Nigeria. *International Journal of Emerging Technologies and Innovative Research (www.jetir.org)*, ISSN:2349-5162, Vol.2, Issue 10, page no.141-145, <https://www.jetir.org/view?paper=JETIR1510026>.



FEATURED PUBLICATIONS

Antioxidant and Dietary Fibre Content of Noodles Produced From Wheat and Banana Peel Flour

This study found that adding banana peel flour to wheat flour can improve the nutritional value of noodles, such as increasing dietary fiber and antioxidant content, while reducing glycemic index.

DOI: <https://doi.org/10.54117/ijjfs.v2i2.24>

Cite as: Oguntoyinbo, O. O., Olumurewa, J. A. V., & Omoba, O. S. (2023). Antioxidant and Dietary Fibre Content of Noodles Produced From Wheat and Banana Peel Flour. *IPS Journal of Nutrition and Food Science*, 2(2), 46–51.

Impact of Pre-Sowing Physical Treatments on The Seed Germination Behaviour of Sorghum (*Sorghum bicolor*)

This study found that ultrasound and microwave treatments can improve the germination of sorghum grains by breaking down the seed coat and increasing water diffusion, leading to faster and more effective germination.

Submit your manuscript for publication: [Home - IPS Intelligentsia Publishing Services](#)

• Thanks for publishing with IPS Intelligentsia.